
Article:
Chau-Khun, M., Awang, A.Z., Omar, W. et al. (3 more authors) (2015) Elastic Design of Slender High-Strength RC Circular Columns Confined with External Tensioned Steel Straps. Advances in Structural Engineering, 18 (9). 1487 - 1499. ISSN 1369-4332

https://doi.org/10.1260/1369-4332.18.9.1487

Chau-Khun, M., Awang, A. Z., Omar, W., Pilakoutas, K., Tahir, M. M., & Garcia, R. (2015). Elastic Design of Slender High-Strength RC Circular Columns Confined with External Tensioned Steel Straps. *Advances in Structural Engineering*, 18(9), 1487-1500. http://dx.doi.org/10.1260/1369-4332.18.9.1487

Elastic design of slender high-strength RC circular columns confined with external tensioned steel straps

Ma Chau Khun[a*], Abdullah Zawawi Awang[a], Wahid Omar[a], Kypros Pilakoutas[b], Mahmood Mohd Tahir[a], Reyes Garcia[b]

[a] Faculty of Civil Engineering, Universiti Teknologi Malaysia, Skudai, Johor, Malaysia
[b] Department of Civil and Structural Engineering, The University of Sheffield, Sheffield, UK

* Corresponding author: machaukhun@gmail.com, abdullahzawawi@utm.my

Tel.: +60 16-8366360

Abstract

This article proposes a design approach to calculate the capacity of slender high-strength concrete (HSC) columns confined with a cost-effective Steel Strapping Tensioning Technique (SSTT). The approach is based on results from segmental analyses of slender SSTT-confined circular columns subjected to eccentric loads. A capacity reduction factor analogue to that proposed by Kwak and Kim (2004) accounts for the effect of slenderness in design. P-M interaction diagrams computed using rigorous nonlinear P-Δ analyses are compared to those calculated by the proposed approach to assess its accuracy. The results indicate that the proposed approach predicts conservatively the ultimate capacity of slender HSC circular columns confined using the SSTT, and therefore it can be used in the design of modern reinforced concrete (RC) structures.

Keywords: High-Strength Concrete; Steel Straps; Confinement; Slender Circular Columns; Ultimate Capacity

1 Introduction

To reduce the building mass and maximise usable floor space, many modern high-rise moment-resisting RC frame buildings are constructed using high-strength concrete (HSC) columns with small cross sections (compared to the column length) and end restraints that cannot prevent column sway. Such "slender columns" tend to deform laterally when subjected to axial load and bending moments, thus subjecting the columns to additional (second order) moments that add to the first order moments. Hence, at large lateral deformations, slender columns can experience global buckling and can fail at lower loads compared to those resisted by "short" columns. To account for the additional second order moments in design, current design codes [e.g. Eurocode 2 (2004), ACI 318 (2011)] factorise the first order moments by an "amplification factor" that essentially depends on the lateral deformation of the slender columns. In these codes, the column lateral deflections are calculated using an approximate flexural stiffness (EI) of the cross section. However, the calculation of EI is not trivial as this value is affected by cracking, time-dependent effects and the nonlinearity of the concrete stress-strain curve as the applied load increases. Moreover, equations to compute EI included in existing codes are applicable to normal-strength concrete (NSC) columns with rectangular cross section, and have proven conservative for the design of circular columns (Bonet et al. 2011). On the other hand, rigorous numerical P-Δ analyses can predict accurately the lateral deformations of slender columns, but such analyses are time-consuming and therefore difficult to use in practice.

To overcome the above drawbacks, Kwak and Kim (2004) proposed a direct capacity reduction method for the design of slender RC columns. In this method, the column is initially assumed as "short", and its load-moment (P-M) interaction diagram is calculated using section analysis based on force equilibrium and compatibility conditions. To compute the ultimate capacity of the slender column, the P-M interaction diagram of the "short" column is factorised by a capacity reduction coefficient that accounts for the effect of slenderness. Kwak and Kim (2004) report that the results from the direct capacity reduction method compare reasonably well with those obtained from rigorous P-Δ analyses of columns with different cross section dimensions, longitudinal steel ratios and slenderness ratios L/r (L=column length; r=ratio of gyration of the column cross section). Moreover, the method predicts more accurately

the capacity of columns with L/r≥70 in comparison to the "amplification factor" method used by ACI 318 (Kwak and Kim 2004).

Previous research indicates that HSC columns can fail in a non-ductile manner, and therefore adequate confinement is necessary to provide ductility (Shin et al. 1989; Ho 1994). Internal steel confinement (ties or stirrups) was used in the past to enhance the ductility of such columns (e.g. Canbay et al. 2006, Ho et al. 2010). However, the effectiveness of internal stirrups at enhancing column ductility is limited as only the inner core of the column cross section is effectively confined after concrete cover spalling occurs, usually close the peak column capacity. To prevent concrete cover spalling and enhance the effectiveness of the confinement, concrete-filled steel tubular (CFST) columns have been examined experimental and analytically in the past (e.g. O'Shea and Bridge 2000; Giakoumelis and Lam 2004; Han et al. 2008; Ho et al. 2014). CFST are an attractive structural solution as the confining steel tubes can be also used as permanent formwork. More recently, externally bonded Fibre Reinforced Polymers (FRP) were also utilised to confine HSC members (e.g. Idris and Ozbakkaloglu 2013; Lim and Ozbakkaloglu 2014). However, both steel tubes and FRP composites can only provide passive confinement to concrete elements. Moreover, the initial cost of FRP may discourage their use as confinement solution in low and medium income developing countries. As a consequence, it is deem necessary to develop more cost-effective confining solutions for RC columns.

Recently, a cost-effective Steel Strapping Tensioning Technique (SSTT) was proven very effective at enhancing the load capacity and ductility of "short" columns cast with NSC (Moghaddam et al, 2010) and HSC (Awang 2013; Awang et al. 2013). The SSTT involves the post-tensioning of high-strength steel straps around RC members using hydraulically-operated steel strapping tools as those utilised in the packaging industry. After post-tensioning, the straps are fastened mechanically using jaws push-type seals to maintain the tensioning force. This provides active confinement to the full section of members, thus increasing their ductility and capacity. In comparison to other confining techniques such as FRP, the SSTT has advantages such as ease and speed of application, ease of removing or replacing steel straps, and low material cost. However, whilst most of the previous studies used the SSTT as a retrofit solution

for existing RC elements (Helal et al. 2014; Garcia et al. 2014), less research has examined its use as external confinement for new HSC columns. Moreover, it is necessary to provide simple design methods for new SSTT-confined HSC columns so that the technique can be widely used in practice.

This paper proposes a design approach for slender HSC circular columns confined using the SSTT. The approach was developed using results from segmental analyses of SSTT-confined circular columns subjected to eccentric loads. A capacity reduction factor analogue to that proposed by Kwak and Kim (2004) accounts for the effect of slenderness that usually dominates the design of such columns. P-M interaction diagrams computed using rigorous nonlinear P-Δ analyses are compared to those calculated using the proposed design approach to assess its accuracy. The design approach proposed in this study is expected to contribute towards a) a wider use of the SSTT in new HSC structures, b) a faster adoption of the cost-effective active confinement technique by designers/practitioners and design guidelines, and c) a significant reduction of computational effort during the design of new HSC structures.

2 Deflections of slender SSTT-confined HSC columns

A theoretical model is proposed to calculate the deflections of slender SSTT-confined HSC columns subjected to eccentric loads. The model simulates the second order effects experienced by a slender column using an axial load-moment curvature path. The load-deflection curve at each discrete point of the column is obtained by a numerical integration method (Newmark 1943). The analyses are carried out using a computational code written in MATLAB 7.6, according to the procedure described in the following sections.

2.1 Constitutive models for analysis

In this study, the confinement model proposed by Awang et al. (2013) is used to account for the effect of steel strap confinement on HSC. The model is based on the equations proposed originally by Mander et al. (1988) for normal strength concrete subjected to active confinement, but Awang et al. (2013) calibrated the model (using an extensive experimental database) and extended its applicability to HSC columns confined with the SSTT. Accordingly, the concrete stress (f_{ci}) at a given strain (ε_{ci}) is defined by:

$$f_{ci} = \frac{f'_{cc} x r}{r - 1 + x^r} \quad (1)$$

where $x=\varepsilon_{cc}/\varepsilon'_{cc}$; ε_{cc} is the axial compressive strain of concrete and is computed as $\varepsilon_{cc}=[1+(5(f'_{cc}/f_{co})-1)]$; ε'_{cc} and f'_{cc} are the strain and concrete strength in confined conditions, respectively; and f_{co} is the unconfined concrete compressive strength. Likewise, $r=E_c/(E_c-E'_{sec})$, where E_c is the tangent modulus of elasticity of concrete and E'_{sec} is the secant modulus of elasticity of the confined concrete at peak stress. For the analysis performed in this study, these values are assumed to be $E_c=22700\sqrt{f'_{cc}/19.6}$ (MPa) and $E'_{sec}=f'_{cc}/\varepsilon'_{cc}$ (MPa), as suggested by Awang et al. (2013),

The values f'_{cc} and ε'_{cc} are calculated using the empirical model proposed recently by Awang et al. (2013) for concrete confined using the SSTT:

$$f'_{cc} = f_{co} \cdot 2.62(\rho_v)^{0.4} \quad (2)$$

$$\varepsilon'_{cc} = \varepsilon_{co} \cdot 11.60(\rho_v) \quad (3)$$

where ρ_v is the volumetric confinement ratio of steel straps ($\rho_v=V_s f_y/V_c f_{co}$, where V_s and V_c are the volumes of straps and confined concrete, respectively, and f_y is the yield strength of the straps); and ε_{co} is the ultimate strain of unconfined HSC (assumed equal to 0.004). It should be mentioned that Eqns 2 and 3 were calibrated using data from uniaxial compressive tests on 140 concrete cylinder specimens (100×200 mm) with strap confinement ratios ranging from 0.06 to 0.86.

A simplified bilinear tensile stress-strain (f_s-ε_s) model is adopted for the reinforcement, according to:

$$\begin{aligned} f_s &= \varepsilon_s E_s \quad \text{for } 0 \le \varepsilon_s \le \varepsilon_y \\ f_s &= f_y \quad \text{for } \varepsilon_s > \varepsilon_y \end{aligned} \quad (4)$$

where E_s is the elastic modulus of the longitudinal column reinforcement; whereas ε_s and ε_y are the strain and yield strain of such reinforcement, respectively.

The moment-curvature relationship of a column can be determined using the above material properties and the geometry of the cross section, as shown in the following section.

2.2 Calculation of moment-curvature relationships

2.2.1 Material properties and section analyses

For the analyses performed in this paper, a column with circular cross section of diameter D=150 mm cast using HSC of f_{co}=60 MPa is assumed (Figure 1a). The longitudinal column reinforcement consists of four 10 mm bars, with a yield strength f_y=460 MPa and an elastic modulus E_s=200 GPa. A free concrete cover of 20 mm is adopted. Each confining steel straps is assumed to have a cross section of 0.5×15 mm and an elastic modulus of 200 GPa. These properties are typical of steel straps used in the packaging industry in Southeast Asia.

To achieve a desired confined concrete strength using the SSTT, designers are free to select the volumetric ratio ρ_v by changing the strap spacing, number of strap layers, yield strength of the straps and compressive concrete strength. However, typical values of ρ_v for practical confining applications on HSC columns range between 0.05 and 0.50. Whilst higher values of ρ_v usually lead to higher column capacity, the number of straps that can be installed is limited by practical aspects such as a) the clear spacing between straps necessary to secure the metal clips using the jaws (minimum 2-3 mm), b) the number of strap layers than can be secured using a single clip (normally no more than two layers of straps), and c) the yield strength of the steel straps. Therefore, SSTT volumetric ratios ρ_v=0.09, 0.25 and 0.50 are used in this study to assess the effect of light, moderate and heavy steel strap confinement that can be applied in practice. Results from compressive tests on short HSC columns confined with such SSTT volumetric ratios indicate that column failure is dominated by a ‘ductile’ behaviour (e.g Lee et al. 2013).

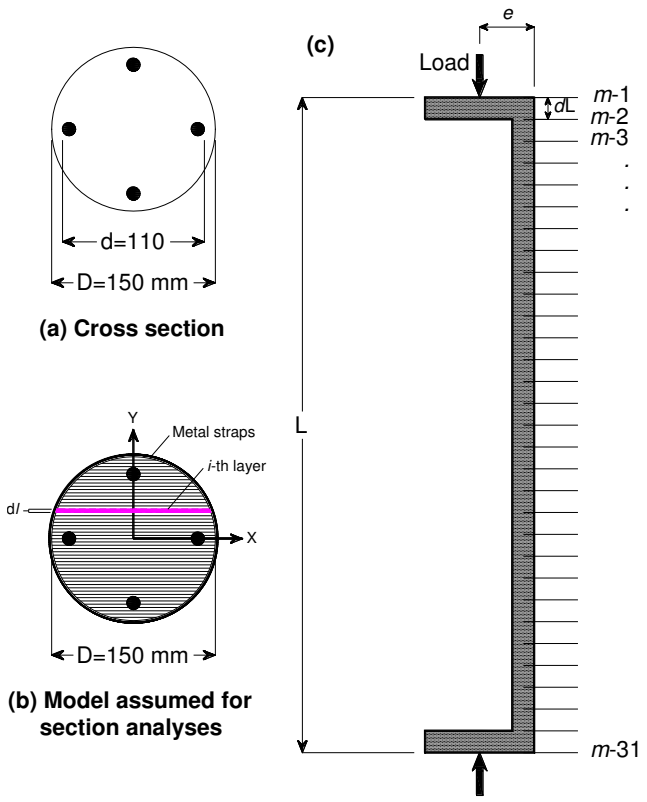

Figure 1. Analytical model and assumptions used in the calculations

Conventional section analysis is carried out by discretizing the column cross section into 50 layers, as shown in Figure 1b. For every step of analysis, the axial load (N_{step}) and bending moment (M_{step}) of the column can be calculated using:

$$N_{step} = \sum_{i=0}^{n} f_{ci} y_i \, dl + (\boldsymbol{\sigma}_{si} - f_{ci}) A_{si} \quad (5)$$

$$M_{step} = \sum_{i=0}^{n} (f_{ci} y_i \, dl) P_i + (\boldsymbol{\sigma}_{si} - f_{ci})(R - d_{si}) A_{si} \quad (6)$$

where y_i is the width of i-th layer; dl is the thickness of each layer (dl=3 mm); $\boldsymbol{\sigma}_{si}$ is the stress of the longitudinal column bar at the i-th layer; A_{si} is the corresponding cross-sectional area of the longitudinal column bar; P_i is the distance from the center point of the i-th layer to the neutral axis; R is the column radius (R=D/2); and d_{si} is the distance between longitudinal tensile bars and the extreme concrete fibre.

2.2.2 Moment-curvature analysis

An incremental iterative procedure is used to calculate the moment-curvature relationships. As such, the extreme fibre concrete strain (ε_{cj}) is increased gradually from zero up to the ultimate concrete strain (ε_{cu}). For each strain value ε_{cj}, the curvature $ø_j$ is varied until the resultant axial load is similar to the applied axial load N_{step}. The neutral axis depth x_n is determined using $ø_j=\varepsilon_{cj}/x_n$, and the resultant moment is thus calculated using Eqn 6.

2.3 Calculation of column deflections

Based on the moment-curvature relationship of the cross section, the lateral deflection of a slender column can be calculated using numerical integration. This technique has been used for the analysis of RC (e.g. Pfrang and Siess 1961; Cranston 1972), steel (Shen and Lu 1983), composite (e.g. Choo et al. 2006; Tikka and Mirza 2006) and FRP-confined columns (e.g. Jiang and Teng 2012).

The curvature of a column (ø) is defined as the second order derivative of its lateral deflection (δ), and its relationship can be expressed using a central difference equation:

$$\delta_{m+1} - 2\delta_m + \delta_{m-1} = -ø_m(\mathrm{d}L^2) \tag{7}$$

where δ_m and $ø_m$ are the lateral displacement and curvature at the m-th discrete point, respectively, whereas m is the discrete point number along the column length (L).

The column model shown in Figure 1c (m=1, 2, 3…31) is used to derive the theoretical results shown later in Section 4. To generate the load-deflection curve, the axial load on the column N_{step} is increased progressively to calculate the corresponding deflection at each discrete point along the column length. The first order moment can be computed as:

$$M_{f,step} = N_{step} \cdot e_m \tag{8}$$

where $M_{f,step}$ and e_m are the first order moment and the eccentricity at the m-th point, respectively. The second order moment ($M_{s,step}$) can be expressed as:

$$M_{s,step} = N_{step} \cdot \delta_m \tag{9}$$

Therefore, the total moment (M_{step}) can be calculated by adding $M_{f,step}$ and $M_{s,step}$:

$$M_{step} = M_{f,step} + M_{s,step} = N_{step} \cdot (e_m + \delta_m) \tag{10}$$

A value δ_2 needs to be assumed to start the calculations, and δ_2=0 is assumed as a first trial. The value for $ø_2$ can be then retrieved from the axial load-moment-curvature relationship once the moment M_2 is calculated. Note that the value M_2 can be calculated using Eqn 10 and assuming δ_2 as equal to zero. Once $ø_2$ and M_2 are known, the value δ_3 of the next discrete point is computed. The lateral deflection of the column can be calculated by repeating the above procedure for subsequent discrete points. However, the lateral deflection is only valid if Eqn 11 is satisfied, i.e. if both ends of the loaded column do not deflect:

$$\delta_1=\delta_{(m+1)} = 0 \tag{11}$$

In the calculations carried out in this paper, the assumed value δ_2=0 resulted in a negative value of $\delta_{(m+1)}$. Therefore, δ_2 was adjusted to a larger value to satisfy Eqn 11. In the analytical P-Δ results shown in Section 4, the solution for the lateral deflection at a given load was halted when the calculated δ_{31} had an absolute value lower than 10^{-4} mm. Full details of the theoretical model and computation procedure are given in Ma et al. (2014).

3 Capacity of short SSTT-confined circular columns

3.1 Development of an equivalent stress block for HSC confined using the SSTT

Current design guidelines for ultimate flexural design of RC members represent the compressive stress profile of concrete using an equivalent stress block with uniform compressive stresses. This equivalent stress block can be defined by: a) the magnitude of stresses, and b) the depth of the stress block. However, the resulting equivalent stress block and the original stress profile must resist the same axial force and bending moment. Due to the steel strap confinement, the equivalent stress block proposed by current design guidelines is inadequate to calculate the ultimate capacity of SSTT-confined HSC columns. Therefore, a parametric study is carried out to develop an equivalent stress block of SSTT-confined HSC sections. The equivalent stress block is defined by:

1) A mean stress factor (α_1), defined as the ratio of the uniform stress over the stress block to the compressive strength of SSTT-confined HSC, and

2) A block depth factor (β_1), defined as the ratio of the depth of the stress block to that of the neutral axis.

To derive α_1 and β_1, section analyses are performed using the circular column model shown in Figure 1b and c. Table 1 summarizes the variables and values considered in the parametric study.

Table 1 Variables and values used in this study

Parameter	Values
x_n	0, 20, 40, 60, 80, 100, 120, 140, 160, 180, 200
ρ_v	0.09, 0.25, 0.5
e_s/D	0.05, 0.1, 0.2, 0.4

The stress distribution over the compression zone of a circular column is examined for the neutral axis depths shown in Table 1. The stress block parameters are determined simultaneously from the axial load and moment equilibrium conditions to match the equations proposed by Macgregor and Wright (2005). For circular columns, the shape of the compression zone is defined by a segment of a circle, as shown in Figure 2.

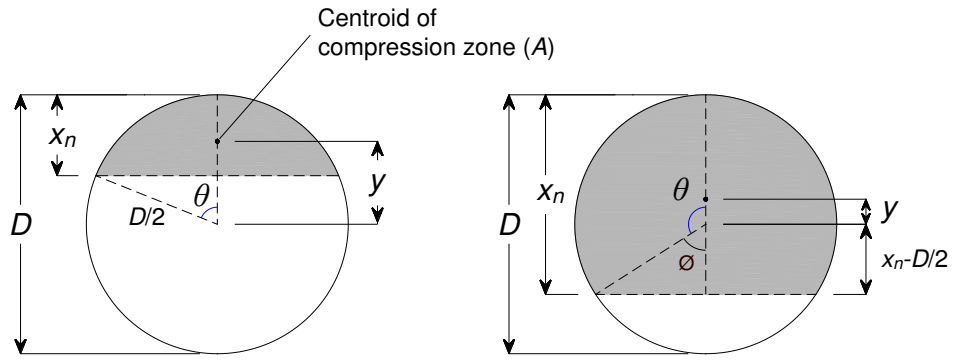

Figure 2 Compression zones of circular columns under eccentric loading (after Macgregor and Wright, 2005)

The area of the compression zone A can be calculated using Eqn 12:

$$A = D^2\left(\frac{\theta_{rad} - sin\theta cos\theta}{4}\right) \quad (12)$$

where θ_{rad} is the angle of the compression zone as defined in Figure 2 (in radians).

The moment of the zone A can be expressed by:

$$Ay = A\left(\frac{D}{2} - \frac{\beta_1 X_n}{2}\right) \quad (13)$$

where y is the distance between the centroid of the compression zone and the centroid of the column; β_1 is the block depth ratio; and x_n is the neutral axis depth (see Figure 2).

The angle θ can be calculated using:

$$\theta = arcos\left(\frac{R-\beta_1 x_n}{R}\right) \quad \text{for } \beta_1 x_n \leq D/2 \tag{14}$$

$$\theta = 180^o - \arccos\left(\frac{\beta_1 x_n - R}{R}\right) \quad \text{for} \quad D/2 \leq \beta_1 x_n \leq D \tag{15}$$

$$\theta = 180^o \quad \text{for } x_n > D \tag{16}$$

where R is the radius of the column.

Therefore, the concrete compressive load (C_c) for a circular column is:

$$C_c = \alpha_1 f'_{cc} A \tag{17}$$

The moment produced by the concrete in compression is given by:

$$M_c = \alpha_1 f'_{cc} Ay \tag{18}$$

For compressive force on the compression reinforcement, the strain of the longitudinal bars (ε_{sc}) can be calculated using strain compatibility:

$$\varepsilon_{sc} = \varepsilon_{cu}\left(1 - \frac{d'}{x_n}\right) \tag{19}$$

where *d'* is the distance from the outermost fibre to the compressive bars; and the rest of the variables are as defined before.

Hence, the compressive stress in the longitudinal bars ($\boldsymbol{\sigma}_{sc}$) can be calculated using Eqn 20 or 21:

$$\boldsymbol{\sigma}_{sc} = E_s \varepsilon_{sc} \quad \text{for } \varepsilon_{sc} \leq \varepsilon_{sy} \tag{20}$$

$$\boldsymbol{\sigma}_{sc} = f_{sy} \quad \text{for } \varepsilon_{sc} > \varepsilon_{sy} \tag{21}$$

where ε_{sy}, f_{sy} and E_s are the yield strain, yield stress and the elastic modulus of the longitudinal column bars.

The compression force of the compression bars can be calculated as a function of the area of compressive steel (A_{sc}):

$$C_s = \boldsymbol{\sigma}_{sc} A_{sc} \tag{22}$$

Similarly, the strain (ε_{st}) and stress ($\boldsymbol{\sigma}_{st}$) in the column tension bars can be calculated as:

$$\varepsilon_{st} = \varepsilon_{cu} \left(\frac{d}{x_n} - 1\right) \quad (23)$$

$$\boldsymbol{\sigma}_{st} = E_s \varepsilon_{st} \; ; \; \varepsilon_{st} \leq \varepsilon_{sy} \quad (24)$$

$$\boldsymbol{\sigma}_{st} = f_{sy} \; ; \; \varepsilon_{st} \geq \varepsilon_{sy} \quad (25)$$

Therefore, the tensile force in the bars is given as:

$$T = \varepsilon_{st} A_{st} \quad (26)$$

Figure 3 shows the stress block factor results obtained from the analysis of SSTT-confined HSC circular columns with different neutral axis depths (x_n). Previous research (Awang 2013) has shown that the SSTT is effective at confining concrete only if ρ_v>0.09, and that values $0 \geq \rho_v \leq 0.09$ can be used to represent unconfined concrete. As a result, the corresponding data results for ρ_v=0.09 are plotted at ρ_v=0 in Figure 3 to obtain a linear distribution. Figure 3a shows that α_1 tends to increase with the volumetric ratio of confining steel straps, ρ_v. Conversely, Figure 3b shows that β_1 varies only slightly for the examined ρ_v ratios, and therefore a constant value can be assumed for practical design:

$$\beta_1 = 0.90 \quad (27)$$

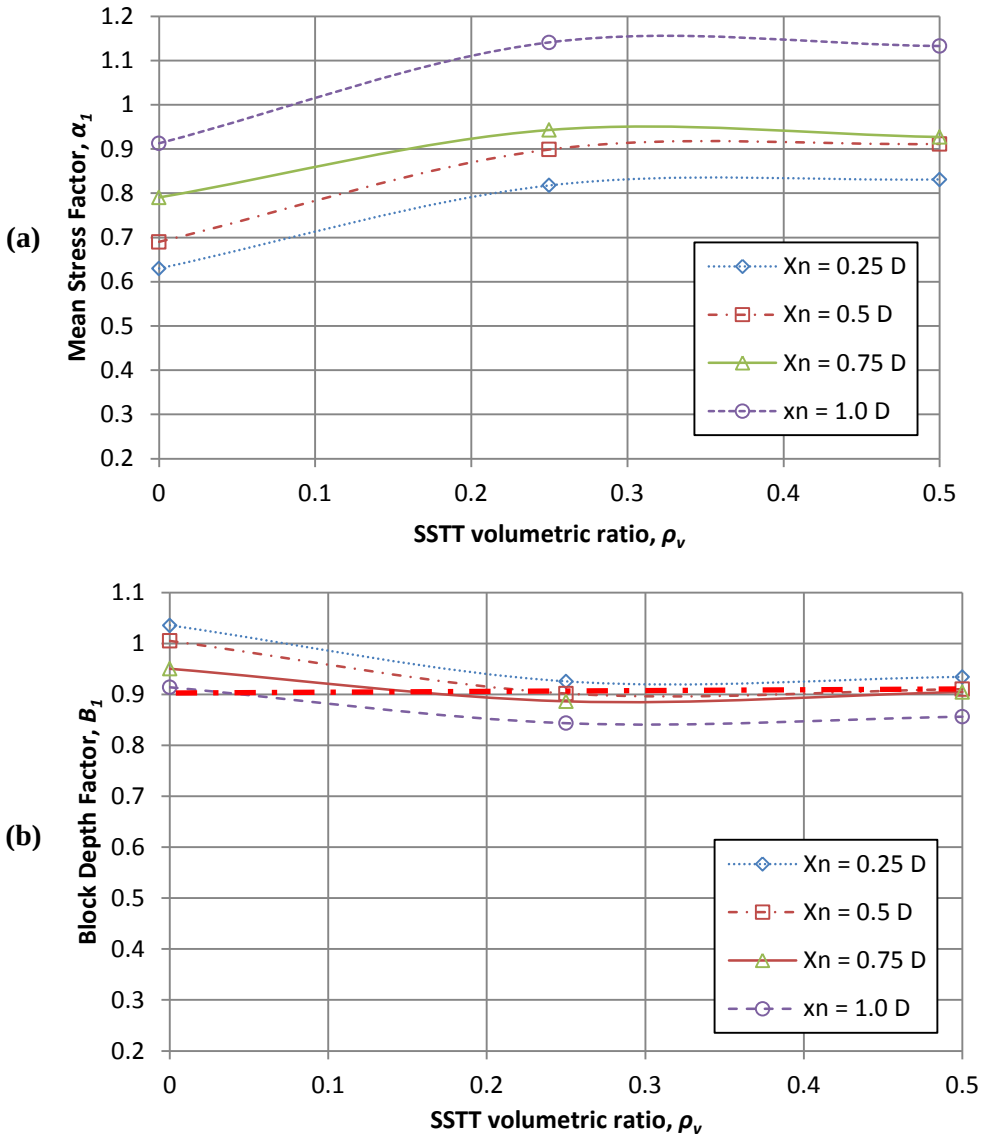

Figure 3 Stress block factors for SSTT-confined HSC sections

Once β_1 is defined, the mean stress factor α_1 can be recalculated using the equivalent stress block approach. Figure 4 shows the recalculated factor α_1, but using a constant value β_1=0.9. Based on regression analysis (see Figure 4), Eqn 26 is proposed to compute α_1:

$$\alpha_1 = 0.195\rho_v + 0.85 \quad (28)$$

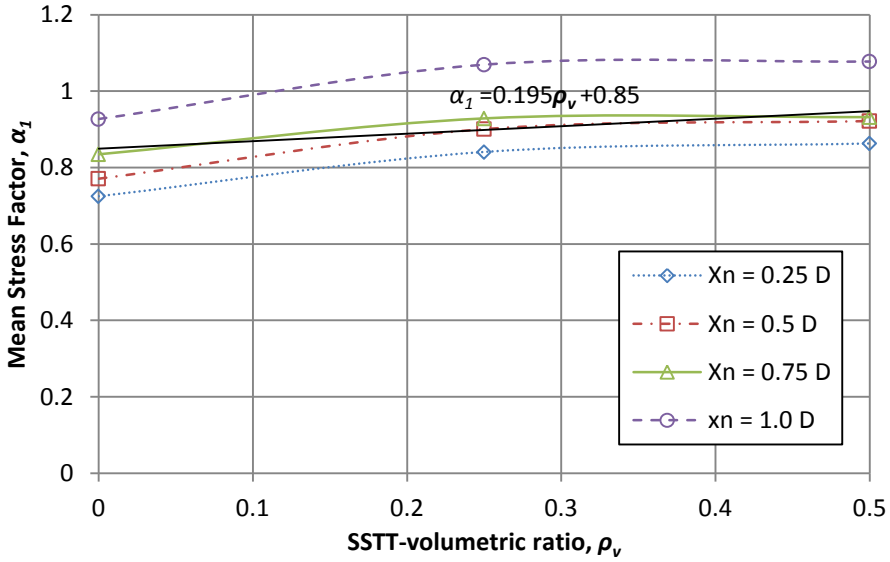

Figure 4 Recalculated mean stress factor α_1 for SSTT-confined HSC sections assuming β_1=0.9

3.2 Ultimate capacity of short SSTT-confined columns

The interaction diagram of a short SSTT-confined HSC column can be developed using Eqns 29 and 30 and the values α_1 (Eqn 28) and β_1=0.90 determined in the previous section:

$$N_u = C_c + C_s + T \tag{29}$$

$$M_u = M_c + C_s\left(\frac{D}{2} - d'\right) + T\left(d - \frac{D}{2}\right) \tag{30}$$

where N_u and M_u are ultimate load and moment capacity of the column; and the rest of the variables are as defined before.

Figure 5 compares the axial load capacity predicted using Eqn 29 and section analyses. The results are shown for values ρ_v=0.09, 0.25 and 0.50, and e/D ratios ranging from 0.05 (minimum eccentricity) to 0.40. It is shown that Eqn 29 predicts the test results with good accuracy (correlation coefficient R^2=0.96).

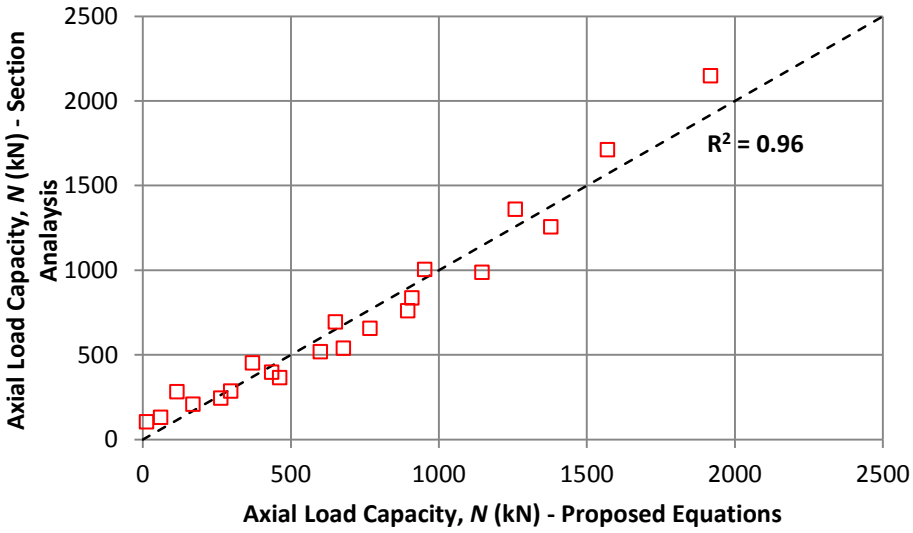

Figure 5 Prediction of design Eqn 29

Figure 6 compares the interaction diagrams calculated using Eqns 29 and 30 and section analysis. The results are shown for ρ_v=0.09, 0.25 and 0.50 and e/D ratios ranging from 0.05to 0.4. It can be seen that the results from Eqns 29 and 30 match reasonably well those from section analysis, although some minor differences are observed for eccentricities close to the balanced eccentricity (e_b). The calculations were halted when the neutral axis depth exceeded the cross-section dimensions (i.e. when $\beta_1 x_n$>150 mm). Overall, Figure 6 indicates that Eqns 29 and 30 can be used to assess the capacity of short SSTT-confined HSC columns. However, columns of modern high-rise RC buildings are typically slender and therefore such slenderness needs to be accounted for in design.

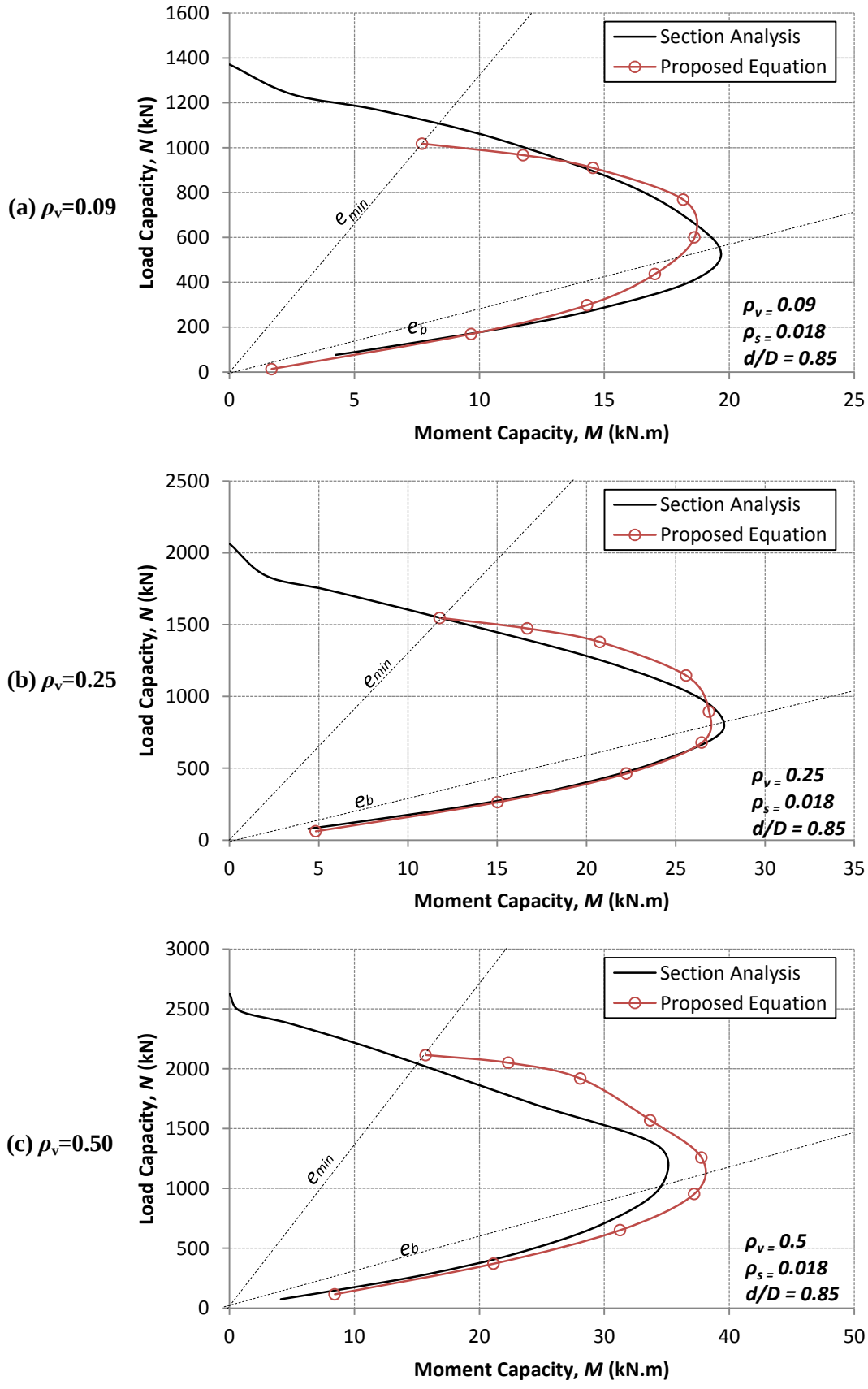

Figure 6 Comparison between interaction diagrams based on section analysis and predictions by Eqns 29 and 30 for (a) ρ_v=0.09, (b) ρ_v=0.25, and (c) ρ_v=0.50

4 Design approach for slender SSTT-confined HSC columns

A new approach is proposed to predict the ultimate capacity of slender SSTT-confined HSC columns, based on the direct capacity reduction method proposed by Kwak and Kim (2004). In this method, the column is initially assumed as "short", and its load-moment (P-M) interaction diagram is calculated using section analysis based on force equilibrium and compatibility conditions. To compute the ultimate capacity of the original slender column, the P-M interaction diagram of the "short" column is factorised by a capacity reduction factor (C) that accounts for the effect of slenderness. C represents the normalised ratio of the difference between the capacities of a "short" and a slender column (see Figure 7), and is defined by:

$$C = 1 - [(0A - 0B) / 0A] \quad (31)$$

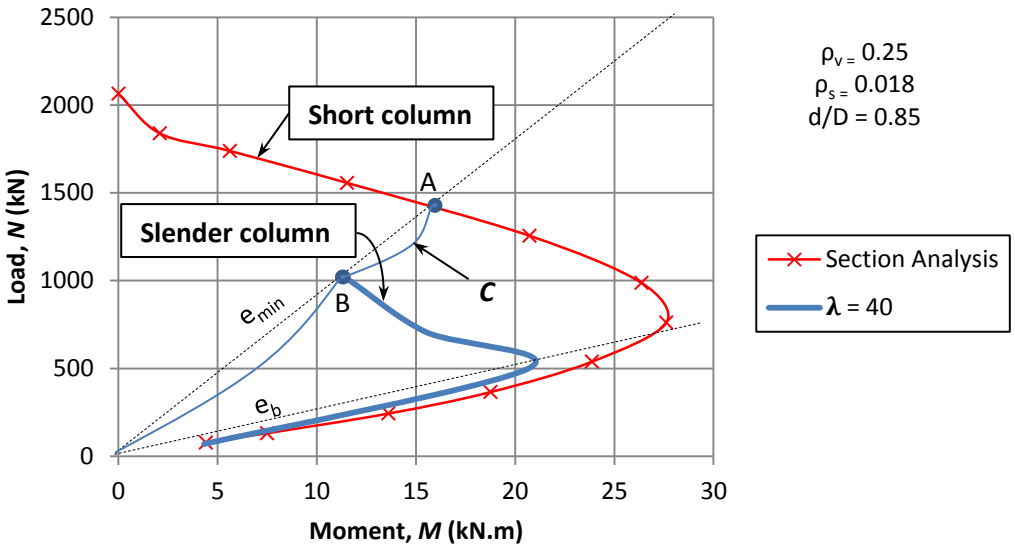

Figure 7 Example of capacity reduction coefficient, C.

4.1 Calculation of the capacity reduction factor *C*

Figure 8 shows results of the numerical analysis performed using the theoretical model described in Section 2 for slenderness ratios λ=20, 30 and 40. The results in this figure indicate that, as expected, second order effects have more influence on the column's behaviour as slenderness ratios increase. This can be attributed to the smaller flexural stiffness of columns with larger slenderness ratios, which increases the lateral deflection and therefore the second order effects. Figure 8 also shows that the second

order effects increase with the eccentricity of the applied axial load N. However, such effects reduce as the value of the eccentricity attains the balanced eccentricity, e_b. Moreover, for eccentricities larger than the balanced eccentricity e_b, the influence of the second order effects reduces further, up to the point of being practically negligible when the applied axial load is close to zero.

Figure 9 shows the calculated capacity reduction factor C for confined columns with slenderness ratios $\boldsymbol{\lambda}$ =20, 30 and 40. It is shown that C increases proportionally with $\boldsymbol{\lambda}$ and ρ_v. The results in Figure 9 also suggest that C reaches a maximum value when the eccentricity is close to the balanced eccentricity.

(a) ρ_v=0.09

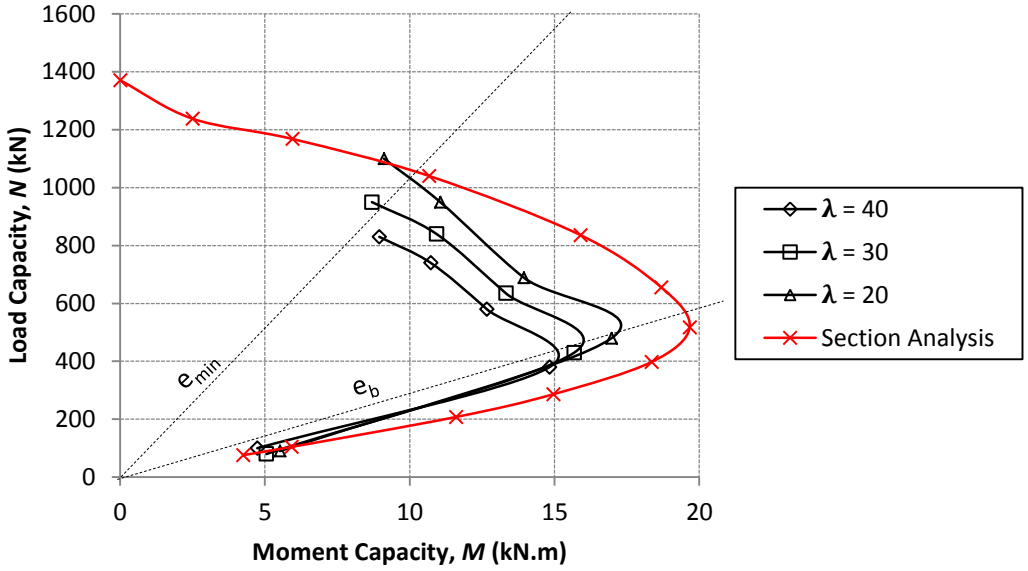

(b) ρ_v=0.25

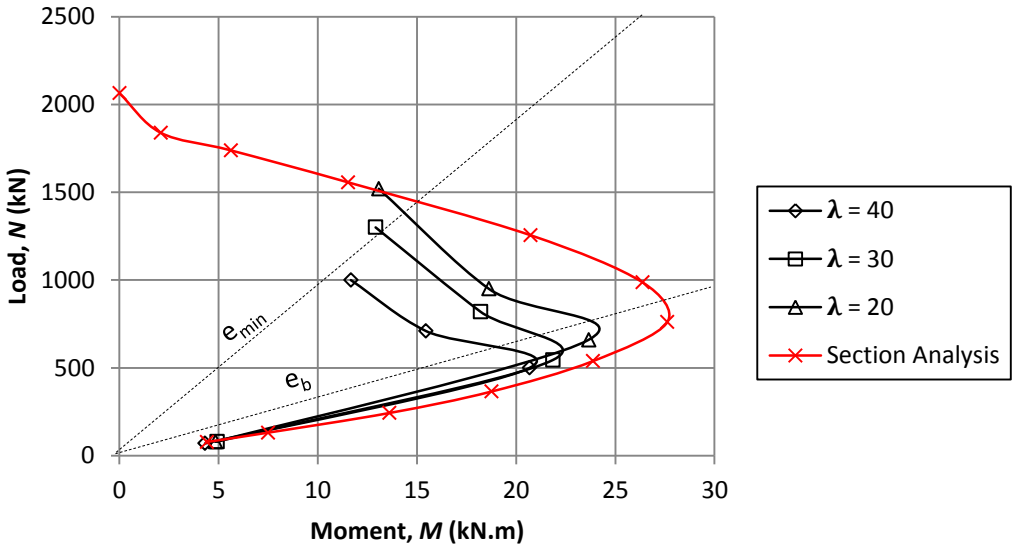

(c) ρ_v=0.50

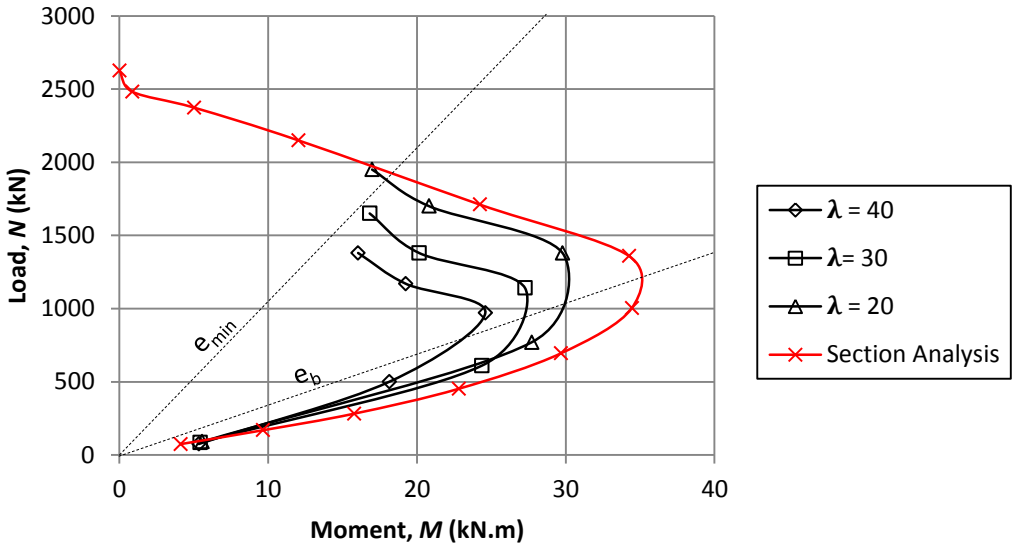

Figure 8 Load-moment interaction diagram developed from the proposed theoretical model for (a) ρ_v=0.09, (b) ρ_v=0.25, and (c) ρ_v=0.50

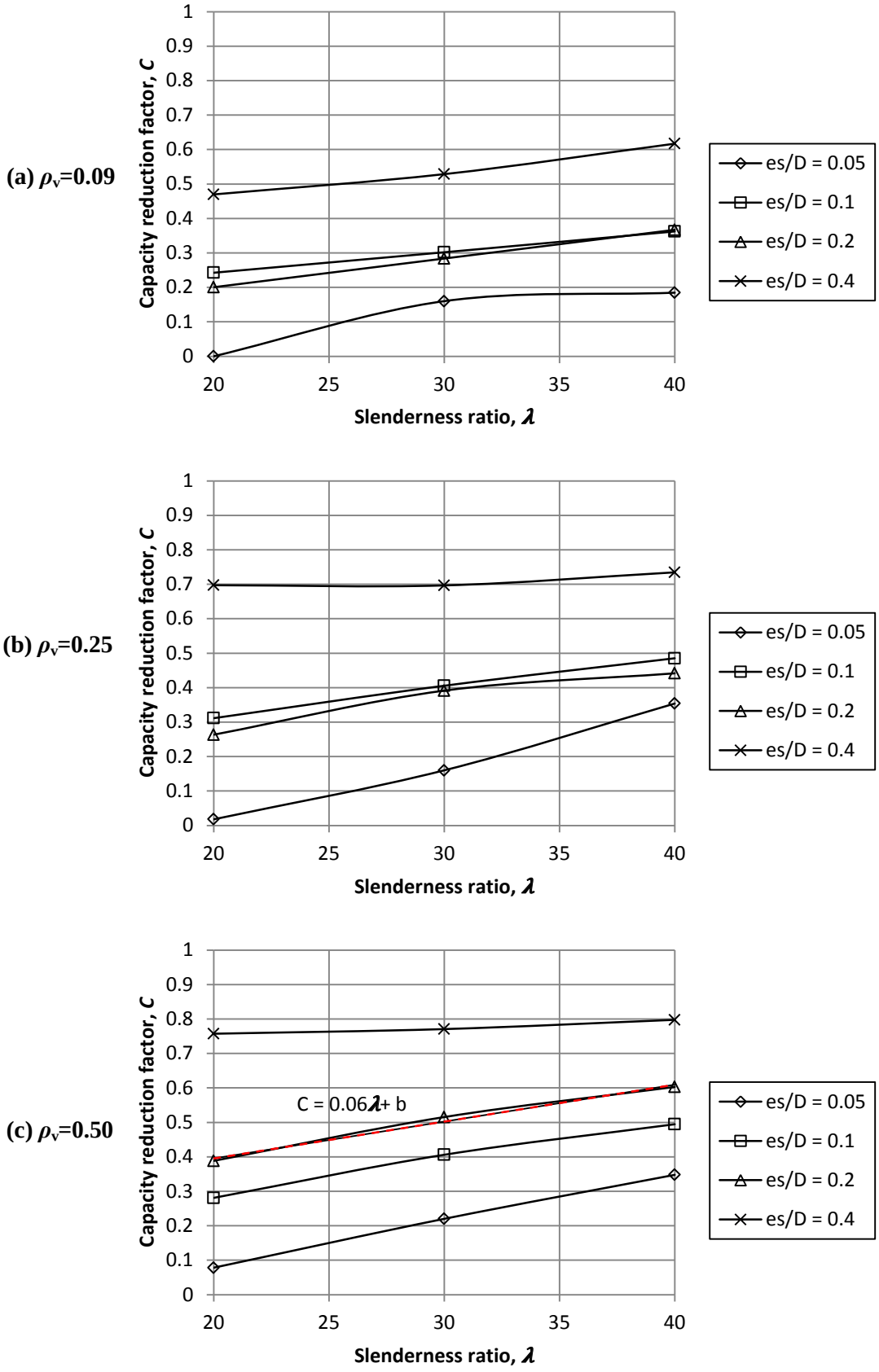

Figure 9 Results of capacity reduction coefficient versus slenderness ratio for (a) ρ_v=0.09, (b) ρ_v=0.25, and (c) ρ_v=0.50

Based on linear regression, two sets of formulas are proposed to compute the capacity reduction coefficient C:

(1) For $e_s<e_b$. Eqn 32 is proposed for columns subjected to an eccentricity smaller than the balanced eccentricity, e_b:

$$C = 0.06\,\lambda + b \quad \text{for } e_s < e_b \tag{32}$$

where b is a coefficient that accounts for the effect of the volumetric ratio of steel strap confinement, ρ_v.

Figure 10 shows the effect of ρ_v on the coefficient b included in Eqn 32. Based on the results of this figure, a linear regression formula is proposed to determine b:

$$b = -0.1\,\rho_v + 0.12 \tag{33}$$

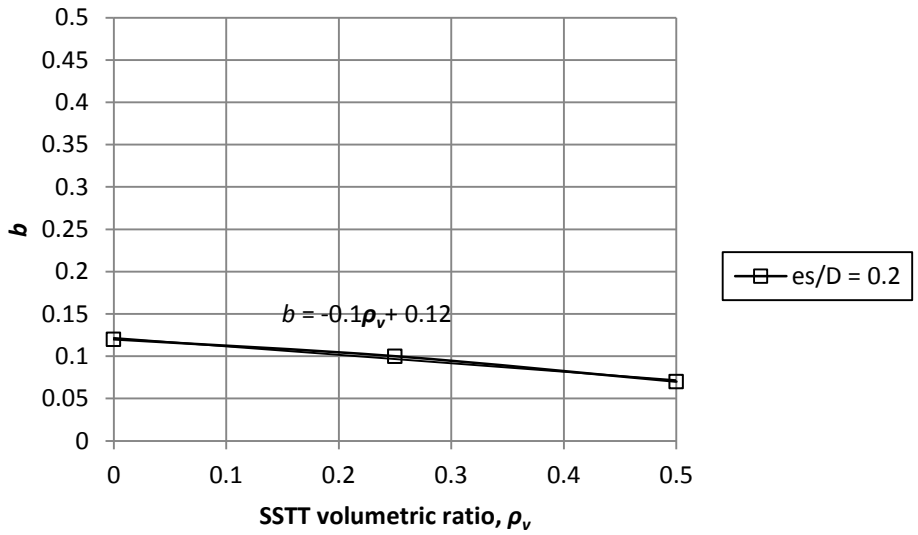

Figure 10 Effect of strap volumetric ratio ρ_v on coefficient b

(2) For $e_s>e_b$. Figure 11 shows that the relationship between the capacity reduction capacity C and the slenderness ratio line is practically linear. As a result, the capacity reduction factor C, for a column with eccentricity larger than the balanced eccentricity is:

$$C = 0.4\,\rho_v + 0.6 \quad \text{for } e_s > e_b \tag{34}$$

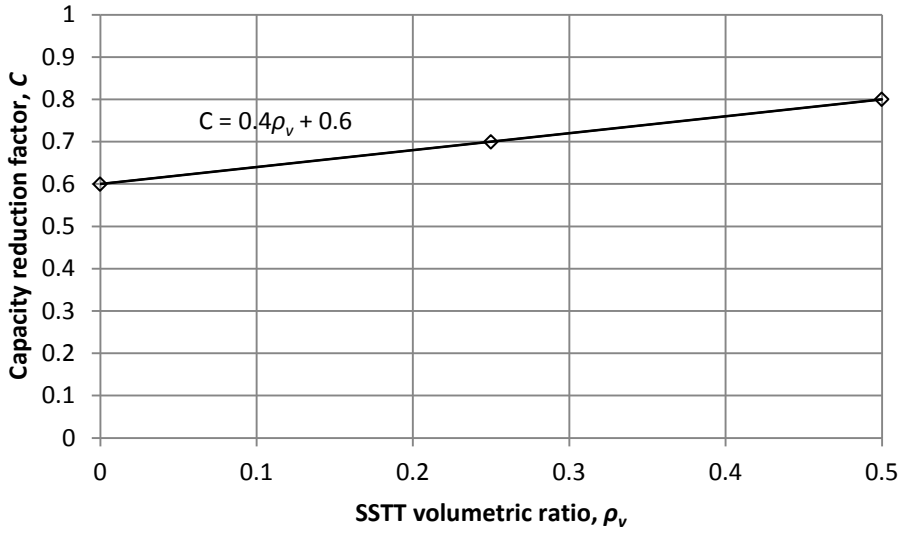

Figure 11 Effect of strap volumetric ratio ρ_v on the capacity reduction factor C

Eqns 32 to 34 were developed based on the upper limit values of the capacity reduction coefficient, C. Note that, for simplicity, the normalised eccentricity, e_s/D is not incorporated in these equations. Hence, the predictions from Eqns 32 to 34 can be very conservative for very small eccentricities. Nonetheless, as shown in the following section, Eqns 32 to 34 are sufficiently accurate to calculate the ultimate capacity of slender SSTT-confined HSC columns.

Based on the results of this section, Eqns 35 and 36 are proposed to calculate the ultimate resisting capacity of slender SSTT-confined HSC columns:

$$N_s = C \cdot N_u \tag{35}$$

$$M_s = C \cdot M_u \tag{36}$$

where the N_s and M_s are the slenderness-factored ultimate load and ultimate moment, respectively, and N_u and M_u are as defined before (see Eqns 29 and 30).

Note that whilst the proposed design approach is applicable for the design of slender SSTT-confined HSC columns with circular cross section, further research is necessary to propose design equations for SSTT-confined columns with rectangular shapes. In the latter case, the PTMS confinement is expected to be less effective at enhancing load capacity as only the corners of the cross section are fully confined by the steel straps (i.e. the confining effect reduces due to ‘parabolic arching action’).

4.2 Validation of the proposed design approach

Figure 12 compares the M-N results calculated using Eqns 35 and 36 with those from rigorous P-Δ analysis obtained using the theoretical model described in Section 2. It is shown that the proposed equations show similar trends as the theoretical results. In particular, a better matching of results is observed for HSC columns with SSTT volumetric ratios ρ_v=0.25 and 0.50. Note that Eqns 35 and 36 predict conservatively the capacity of unconfined HSC columns, and such conservativeness is higher when the column is subjected to very small eccentricity.

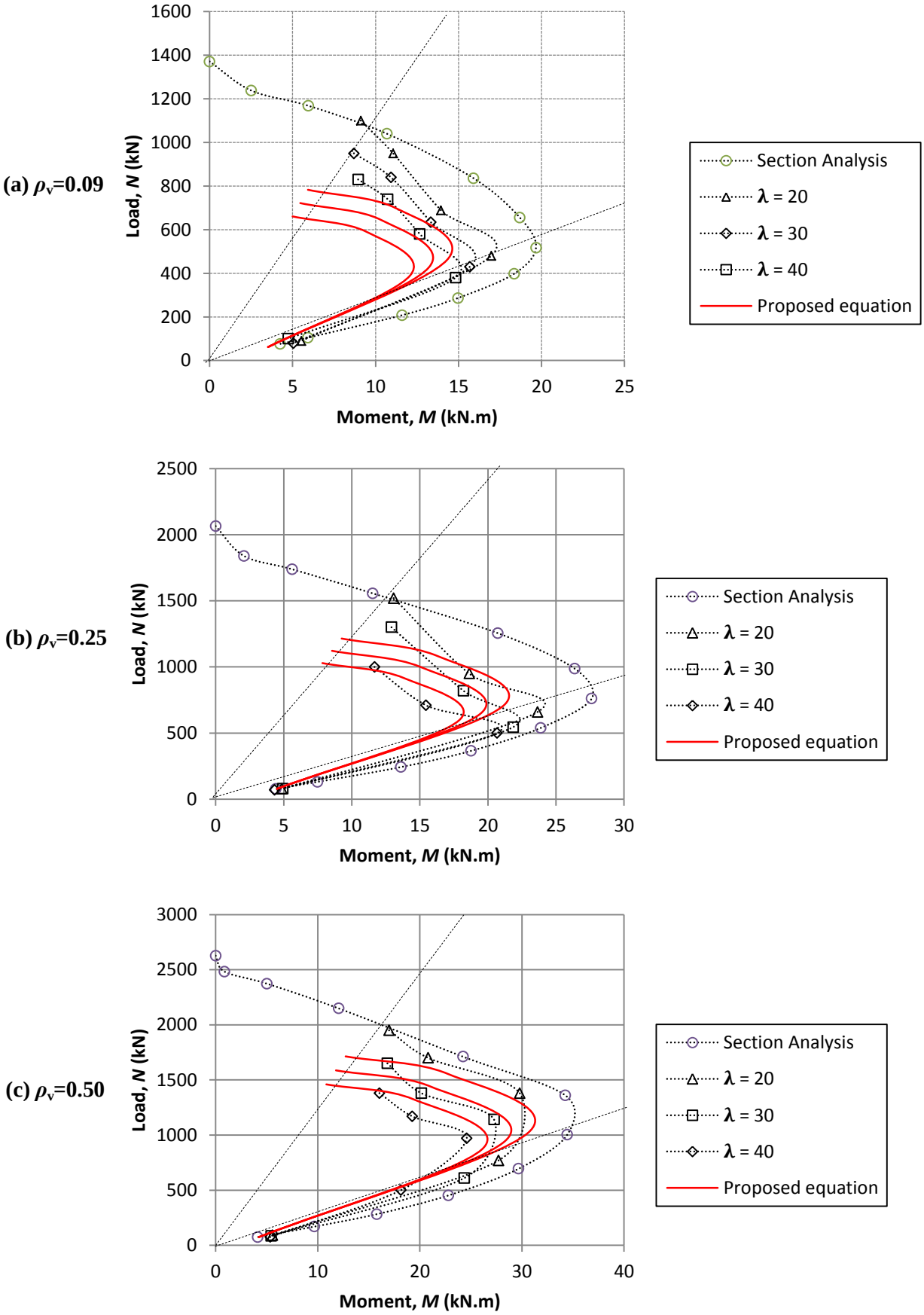

Figure 12 Comparison of results given by Eqns 35 and 36 and theoretical P-Δ analysis

Table 2 compares the predictions given by Eqns 35 and 36 with experimental results (ultimate axial load N_u, and flexural moment M_u) obtained from 18 slender SSTT-confined HSC columns tested recently by Ma et al. (2014). Fifteen of such columns were confined with one or two layers of metal straps placed at clear spacings of 20 or 40 mm, thus leading to confinement ratios ranging from 0.076 to 0.178. The columns had circular sections with diameter D=150 mm, slenderness ratios λ=16, 24 or 40 and were cast using HSC with mean compressive concrete strength f_{co}=62.3-65.5 MPa. The results in Table 2 confirm that the proposed approach predicts conservatively the ultimate capacity of slender SSTT-confined HSC columns, with mean Test/Prediction ratios for axial load (N_u/N_s) and flexural moment (M_u/M_s) equal to 1.31 and 1.10, respectively. The standard deviation of the Test/Prediction ratios (SD=0.22) also indicates the relatively low scatter of the predictions. Based on the results of this study, it is proposed to use Eqns 35 and 36 for the design of practical SSTT confinement solutions for slender HSC columns.

Table 2 Comparison of predictions given by Eqns 35-36 with test results by Ma et al. (2014)

Column ID	**No. of strap layers**	**λ**	**f_{co} (MPa)**	**N_u (kN)**	**N_s (kN)**	**M_u (kNm)**	**M_s (kNm)**	**N_u/N_s (-)**	**M_u/M_s (-)**
C600-E25-R0-C	0	16	65.5	727	570	18.6	14.5	1.28	1.28
C600-E25-R0-S0.076	1	16	65.5	605	570	15.4	14.5	1.06	1.06
C600-E25-R0-S0.12	1	16	65.5	860	635	22.2	23.3	1.35	0.95
C600-E25-R0-S0.178	2	16	65.5	1020	740	28.2	26.8	1.38	1.05
C600-E25-R1-S0.12	1	16	65.5	835	580	21.6	22.3	1.44	0.97
C600-E50-R0-S0.12	1	16	66.7	604	334	30.5	18.7	1.81	1.63
C900-E25-R0-C	0	24	66.7	705	570	18.4	14.9	1.24	1.24
C900-E25-R0-S0.076	1	24	66.7	830	570	22.0	21.2	1.46	1.04
C900-E25-R0-S0.12	1	24	66.7	825	635	21.9	24.0	1.30	0.91
C900-E25-R0-S0.178	2	24	66.7	950	740	25.6	27.3	1.28	0.94
C900-E25-R1-S0.12	1	24	66.7	774	550	21.7	22.3	1.41	0.97
C900-E50-R0-S0.12	1	24	66.7	511	325	26.5	19.1	1.57	1.39
C1200-E25-R0-C	0	32	62.3	565	560	15.4	15.6	1.01	0.99
C1200-E25-R0-S0.076	1	32	62.3	870	560	23.3	15.6	1.55	1.50
C1200-E25-R0-S0.12	1	32	62.3	810	630	22.6	24.6	1.29	0.92
C1200-E25-R0-S0.178	2	32	62.3	832	730	22.4	28.7	1.14	0.78
C1200-E25-R1-S0.12	1	32	62.3	517	500	16.0	15.4	1.03	1.04
C1200-E50-R0-S0.12	1	32	62.3	341	340	18.3	16.7	1.00	1.09
Mean								1.30	1.10

SD	0.22	0.22

It should be mentioned that whilst this study focuses on the design and capacity of SSTT-confined HSC elastic columns, the technique is expected to increase considerably the columns' ductility during the plastic stage. Therefore, further experimental and analytical research is necessary to extend the proposed design method to columns where yielding of the longitudinal reinforcement (or concrete crushing failure) can occur. It should be also noted that creep and shrinkage developing during the design life of the RC column may (slightly) reduce the post-tensioning stress in the steel straps. Accordingly, further tests should investigate the long-term behaviour of the SSTT methodology. However, unlike other permanent confining techniques also affected by creep and shrinkage (e.g pre-cured FRP tubes or concrete-filled steel tubular (CFST) columns), the steel straps can be inspected/assessed over the design life of the column and easily replaced with new straps if stress relaxation is evident.

5 Conclusions

This paper proposes a design procedure to calculate the capacity of slender HSC circular columns confined using a cost-effective Steel Strapping Tensioning Technique (SSTT). To account for the effect of slenderness in the design, the procedure uses a capacity reduction factor, C, analogue to that proposed by Kwak and Kim (2004). From the analyses and results shown in this paper, the following conclusions are drawn:

1) An equivalent stress block for SSTT-confined HSC columns with circular section is developed. The equivalent stress block is defined by a constant block depth ratio (β_1=0.9) and a mean stress factor α_1 that depends on the amount of steel strap confinement (ρ_v). The equivalent stress block predicts the ultimate capacity of "short" SSTT-confined HSC columns with good accuracy.

2) Based on regression analyses, a capacity reduction coefficient, C, is proposed to calculate the capacity of slender SSTT-confined HSC columns with circular cross section. The coefficient was found to depend on the eccentricity level applied on the column, the amount of steel strap confinement and the column slenderness.

3) The proposed design approach is faster than rigorous theoretical P-Δ analysis and predicts conservatively the capacity of slender SSTT-confined HSC columns. Overall, better predictions were obtained for columns subjected to eccentricities larger than the balanced eccentricity, e_b. The proposed equations were effective at predicting conservatively the experimental results of SSTT-confined columns, with Test/Prediction ratios for axial load and flexural moment equal to 1.31 and 1.10, respectively. Therefore, the proposed equations can be used to estimate the ultimate resisting capacity of column during design.

4) Whilst the SSTT has proven effective at enhancing the capacity and behaviour of HSC columns, further research should investigate a) its effectiveness at enhancing the columns' ductility when yielding of the longitudinal reinforcement (or concrete crushing failures) can occur, and b) creep and shrinkage effects on the long-term behaviour of the SSTT methodology. Moreover, it is also necessary to propose design equations for SSTT-confined HSC columns with non-circular cross sections.

Notation

The following symbols are used in this article:

A_{si} = corresponding cross-sectional area of longitudinal steel bar

A_{st} = total cross-sectional area of longitudinal bars

b = coefficient that accounts for the effect of SSTT-volumetric ratio, ρ_v

C = capacity reduction coefficient

D = diameter of column section

dl = thickness of each layer of discretized column section

dL = length of column segmented unit

d_{si} = location of longitudinal tensile bar from the extreme concrete fibre

e = load eccentricities

e_s = column end eccentricities which can be either positive or negative value

E_c = tangent modulus of elasticity of concrete

E'_{sec}= secant modulus of confined concrete at peak stress

E_s = elastic modulus of steel

ε_{co} = ultimate strain of unconfined HSC

ε'_{cc} = peak strain of confined concrete

ε_s = steel strain

ε_y = yield strain of steel

ε_{ci} = concrete strain

ε_{cc} = axial compressive strain of concrete

f_{ci} = concrete stress at a given strain

f_{co} = concrete compressive strength

f_y = yield strength of steel

L = column length

M_{step} = bending moment at progressively incremental loading steps

$M_{f,step}$ = first order moment at a given load step

$M_{s,step}$ = second order moment at a given load step

N_{step} = axial load at progressively incremental loading steps

N_{ult} = ultimate load capacity of column under concentric load

R = radius of column section

V_s = volume of steel straps using the SSTT

V_c = volume of concrete

x = ratio of axial compressive strain to concrete peak strain

x_n = neutral axis depth

y_i = width of i-th layer

ρ_v = confinement volumetric ratio of steel straps

ρ_s = internal reinforcement ratio of column

δ_m = lateral deflection at a discrete point of a column

δ = lateral deflection

ø = curvature

σ_{si} = stress of longitudinal bar at i-th layer

$\boldsymbol{\lambda}$ = slenderness ratio

References

ACI-318 (2011). “Building code requirement for structural concrete and commentary”, ACI Committee 318, American Concrete Institute, Farmington Hill, VA.

Awang AZ, Omar W, Khun MC, Liang M. (2013). “Design of short SSTT-confined circular HSC columns”, International Journal of Research in Engineering and Technology, Vol. 2, No. 8, pp. 331-336.

Awang, A.Z. (2013) “Stress-strain behavior of high-strength concrete with lateral pre-tensioning confinement”, PhD thesis, Universiti Teknologi Malaysia, Malaysia.

Bonet, J. L., Romero, M. L. and Miguel, P.F. (2011). “Effective flexural stiffness of slender reinforced concrete columns under axial forces and biaxial bending”, Engineering Structures, Vol. 33, No. 3, pp. 881-893.

Canbay, E., Ozcebe, G. and Ersoy, U. (2006). ”High-strength concrete columns under eccentric load”, Journal Structural Engineering, Vol. 132, No. 7, pp. 1052–1060.

CEN (2004). “Eurocode 2: Design of concrete structures, Part 1: general rules and rules for building”, European Committee for Standardisation, Brussels.

Choo, C.C., Harik, I.E. and Gesund, H. (2006). “Strength of rectangular concrete columns reinforced with fiber-reinforced polymer bars”, ACI Structural Journal, Vol. 103, No. 3, pp. 452-459.

Cranston, W.B. (1972). “Analysis and design of reinforced concrete columns”, Research Report 20, Cement and Concrete Association, UK.

fib (2013). “Model Code for Concrete Structures 2010”, 1st Ed. Berlin, Germany: Ernst & Sohn GmbH & Co.

Garcia, R., Hajirasouliha, I., Guadagnini, M., Helal, Y., Jemaa, Y., Pilakoutas, K., et al. (2014). “Full-scale shaking table tests on a substandard RC building repaired and strengthened with Post-Tensioned Metal Straps”, Journal Earthquake Engineering, Vol. 18, No. 2, pp.187-213.

Giakoumelis, G., and Lam, D. (2004). “Axial capacity of circular concrete-filled tube columns”, Journal of Constructional Steel Research, Vol. 60, No. 7, pp. 1049-1068.

Han, L.H., Liu, W., and Yang, Y.F. (2008). “Behavior of thin walled steel tube confined concrete stub columns subjected to axial local compression”, Thin-Walled Structures, Vol. 46, No. 2, pp. 155-164.

Helal, Y., Garcia, R., Pilakoutas, K., Guadagnini, M. and Hajirasouliha, I. (2014). “Strengthening of short splices in RC beams using Post-Tensioned Metal Straps”, accepted for publication in Materials and Structures, DOI: 10.1617/s11527-014-0481-6.

Ho, J.C.M., Lai, M. H., and Luo, L. (2014). “Uniaxial behaviour of confined high-strength concrete-filled-steel-tube columns”, Proceedings of the ICE - Structures and Buildings, Vol. 167, No. 9, pp. 520-533.

Ho, J.C.M., Lam, J.Y.K. and Kwan, A.K.H. (2010). “Effectiveness of adding confinement for ductility improvement of high-strength concrete columns”, Engineering Structures, Vol. 32, No. 3, pp. 714–725.

Idris, Y. and Ozbakkaloglu, T. (2013). ”Seismic behavior of high-strength concrete-filled FRP tube columns”, Journal Composites Construction, Vol. 17, No. 6, December 2013: 04013013.

Jiang, T. and Teng, J.G. (2012). “Behavior and design of slender FRP-confined circular RC columns”, Journal of Composites for Construction, Vol. 16, No. 6, pp. 650-661.

Kwak, H.G., and Kim, J.K. (2004). “Ultimate resisting capacity of slender RC columns”, Computers and Structures, Vol. 82, No. 11-12, pp. 901-915.

Lee, H.P., Awang, A.Z. and Omar, W. (2014). “Steel strap confined high strength concrete under uniaxial cyclic compression”, Construction and Building Materials, Vol. 72, 15 December 2014, pp. 48-55.

Li, B., Park, R. and Hitoshi, T. (1994). “Strength and ductility of reinforced concrete members and frames constructed using high strength concrete”, Report 94-5, Christchurch, N.Z., University of Canterbury, Dept. of Civil Engineering, Research Report 0110-3326, 373 pp.

Lim, J.C. and Ozbakkaloglu, C. (2014). “Confinement model for FRP-confined high-strength concrete”, Journal Composites Construction, Vol. 18, No. 4, August 2014: 04013058.

Ma, C.K., Awang, A.Z. and Omar, W. (2014). “New theoretical model for SSTT-confined HSC columns”, Magazine of Concrete Research, Vol. 66, No. 13, pp. 674-684.

Ma, C.K., Awang, A.Z., Omar, W., and Maybelle, L. (2014). "Experimental tests on SSTT-confined HSC columns", Magazine of Concrete Research, Vol. 66, No. 21, pp. 1084-1094.

Macgregor, J.G. and Wright, J.K. (2005). "Reinforced concrete: Mechanics and design", 4th edition, Prentice Hall, New Jersey.

Mander, J.B., Priestely, M.J.N. and Park, R. (1988). "Theoretical stress-strain model for confined concrete", Journal of Structural Engineering, Vol. 114, No. 8, pp. 1805-1826.

Moghaddam, H., Samadi, M., Pilakoutas, K., Mohebbi, S. (2010). "Axial compressive behavior of concrete actively confined by metal strips: Part A: experimental study", Materials and Structures, Vol. 43, No. 10, pp. 1369 -1381.

Newmark, N.M. (1943). "Numerical procedure for computing deflections, moments, and buckling loads." ASCE Transactions, Vol. 108, pp. 1161-1234.

Omar W., Pilakoutas, K and Awang, A,Z,, (2006) "Preliminary experimental investigation on the performance of laterally confined high-strength concrete columns using steel straps", Proc. of the 2nd Asian Concrete Federation Conference, 20-21 November, Bali.

O'Shea, M. and Bridge, R. (2000). "Design of circular thin-walled concrete filled steel tubes", Journal of Structural Engineering, Vol. 126, No. 11, pp. 1295–1303.

Pfrang, E.O. and Siess, C.P. (1961). "Analytical study of the behavior of long restrained reinforced concrete columns subjected to eccentric loads", Structural research series No.214, University of Illinois, Urbana, IL.

Shen, Z.Y. and Lu, L.W. (1983). "Analysis of initially crooked, end restrained steel columns", Journal of Constructional Steel Research, Vol. 3, No. 1, pp. 10-18.

Shin S.W., Ghosh S.K. and Moreno J. (1989). "Flexural ductility of ultra-high strength concrete members", ACI Structural Journal, Vol. 86 No. 4, pp. 394-400.

Tikka, T.M. and Mirza, S.A. (2006). "Nonlinear equation for flexural stiffness of slender composite columns in major axis bending", Journal of Structural Engineering, Vol. 132, No. 3, pp. 387-399.